

Simulations of dynamical stabilization of Ag–Cu nanocomposites by ion-beam processing

R. A. Enrique

Department of Materials Science and Engineering, University of Michigan, Ann Arbor, Michigan 48103

K. Nordlund

Accelerator Laboratory, P.O. Box 43, 00014 University of Helsinki, Finland

R. S. Averback and P. Bellon

Frederick Seitz Materials Research Laboratory and Department of Materials Science and Engineering, University of Illinois at Urbana-Champaign, Urbana, Illinois 61801

(Received 9 August 2002; accepted 3 December 2002)

Recent theoretical results indicate that ion-beam mixing can be used to synthesize nanocomposite structures from immiscible elements, relying on a self-organization phenomenon at steady state under irradiation. According to this modeling, self organization requires that the range of the forced atomic relocations in displacement cascades exceeds a critical value. Experimental evidence supporting the formation of nanocomposites by this mechanism has been found in the immiscible system Ag–Cu irradiated with 1 MeV Kr ions. To address this experimentally relevant model system, and to test the theoretical predictions, we study, by molecular dynamics (MD), the characteristics of irradiation mixing in a Ag–Cu alloy subjected to bombardment with 62 keV He, 270 keV Ne, 500 keV Ar, and 1 MeV Kr ions. The distribution of atomic relocations measured by MD is then used to perform lattice kinetic Monte Carlo (KMC) simulations of phase evolution, during which both thermal decomposition and irradiation mixing operate simultaneously. The KMC results show that, in the framework of this self-organization mechanism, a nanocomposite structure can be stabilized at steady state by irradiation with heavy ions (Ne, Ar, and Kr), but not with He ions. As the characteristic relocation range for He ions is half of that measured for the heavy ions, these results support the theoretical prediction of the existence of a critical relocation range for compositional patterning to take place under irradiation. © 2003 American Institute of Physics. [DOI: 10.1063/1.1540743]

I. INTRODUCTION

Nanocomposite materials provide many opportunities for synthesizing materials with improved or unique properties.^{1,2} The challenge for exploiting this potential, however, resides in the difficulty in synthesizing these ultrasmall objects in a controllable manner. An attractive approach to overcome this difficulty employs a spontaneous self-organization of the composition field of a material during its processing, that is, a self-organized compositional patterning. Indeed, using generic atomistic simulations and analytic modeling we predicted that such dynamical stabilization of compositional patterns could take place in immiscible alloys processed by repeated shear deformation³ or by bombardment with energetic ion beams.^{4,5} Our recent experimental work has validated some of these predictions, as Ag–Cu nanocomposites have been directly synthesized by ball milling,^{6,7} and by irradiation with 1 MeV Kr ions.⁸ Ag–Cu was used in these studies since it is a model immiscible binary alloy with a moderate heat of mixing and little solubility in the terminal phases, and it can be rendered miscible by nonequilibrium methods at low processing temperatures (typically room temperature and below).^{9–11} Heinig *et al.*¹² have independently predicted that precipitates in materials processed by ion beams may undergo inverse coarsening,

and Schmidt *et al.*¹³ and Rizza *et al.*¹⁴ have applied this idea to the synthesis of metallic nanoclusters in SiO₂.

The stabilization of nanocomposites by ion beams results from the dynamical competition between short-range thermally activated atomic jumps, which promote decomposition in an immiscible alloy system, and medium- or long-range forced displacements, which promote composition homogenization. While the formation of nanocomposites during ion irradiation was discussed and possibly even observed decades ago,¹⁵ our recent modeling and simulation work^{4,5} indicates that a critical parameter necessary for compositional self-organization is the range R of the atomic relocations forced by the nuclear collisions between the energetic ions and the atoms of the target material. It is predicted that when R is below a critical value R_c patterning cannot take place, while when $R > R_c$, patterning becomes possible under appropriate irradiation conditions, involving specimen temperature and irradiation flux. The conditions necessary for patterning have been summarized in a dynamical phase diagram as shown, for instance, in Fig. 3 of Ref. 4.

In past work,⁵ the atomic displacements, or relocations, produced by energetic collisions were modeled by swapping two atoms chosen randomly, separated by a distance dictated by a Gaussian distribution. The displacement distribution for ion irradiation, however, is far more complex, and depends

on the ion mass and energy. To determine whether a particular irradiation condition will lead to compositional patterning, it is therefore necessary to consider its actual atomic displacement field. Here, we perform this analysis for irradiation of $\text{Ag}_{50}\text{Cu}_{50}$ with 62 keV He, 270 keV Ne, 500 keV Ar, and 1 MeV Kr ions. As we will show, Ne, Ar, and Kr lead to patterning, but He does not. The results show, moreover, that to a first approximation the mean displacement of atoms provides a good evaluation on whether patterning will occur. Note that throughout this work we use the terms displacement field and displacement distribution to refer to the relocation of atoms in displacement cascades. This displacement distribution thus corresponds to what is often called replacement in the specialized literature, and should not be confused with the Frenkel pairs created by energetic collisions.

To study the effect of the displacement distribution, we combine several atomic simulations techniques. For a given energetic ion, the primary recoil spectrum is calculated using a molecular dynamics range calculation code MDRANGE.¹⁶ Full molecular dynamics (MD) simulations are then performed at various recoil energies in order to sample the primary recoil spectrum, and to calculate the spectrum-averaged distribution of atomic relocation distances. This distribution of atomic relocations is then employed as an input parameter in rigid lattice kinetic Monte Carlo (KMC) simulations, which are used to follow the long-time behavior of the composition of the material during ion-beam processing. Four different ions are considered: 62 keV He, 270 keV Ne, 500 keV Ar, and 1 MeV Kr. The projected range is the same in all cases, 260 nm. These energies have been chosen to maximize the nuclear stopping power in Ag-Cu. As the mass of the incoming ions increases, the forced atomic mixing produced by nuclear collisions should increase, and it is expected that this will favor the stabilization of compositional patterns in the irradiated film.

II. SIMULATION METHODS

We describe here the simulation methods and the parameters used in the simulations. As these methods are standard ones, only a brief summary is given for each procedure, with references for additional information.

A. Primary recoil spectra and molecular dynamics simulations

Primary recoil spectra are calculated using MDRANGE with the ions impacting perpendicular to a randomly chosen plane and therefore correspond to a polycrystalline sample, assuming a random fcc crystal structure. We perform MD simulations of the full evolution of collision cascades produced in the $\text{Ag}_{50}\text{Cu}_{50}$ random fcc alloy by self-recoils in the bulk with energies of 300 eV, 1 keV, 3 keV, 10 keV, and 50 keV, and random initial directions. The simulations utilize the original embedded-atom method potentials of Foiles,¹⁷ which have been found suitable for describing noble metals.¹⁸ The MD cascade simulation methods have been presented elsewhere.¹⁹ The atomic relocation distributions obtained with full MD for all the energies are then summed with the weight factors determined from the MDRANGE calculations.

B. Kinetic Monte Carlo simulations

KMC simulations are employed to follow the long-term evolution of an immiscible binary alloy under the competition of two dynamics: vacancy-assisted thermal diffusion trying to bring the system to equilibrium, and athermal atomic relocations creating random mixing. Although it would be desirable to perform the KMC simulations on a relaxed lattice using the same interatomic potentials as those used in the MD simulations, such a seamless combination of MD and KMC is excessively demanding in terms of computing time. Currently such a method is limited to a few hundred vacancy jumps per atom for systems comprised of a few hundred atoms.²⁰ These limitations are unacceptable for the present task, as unambiguous determination of nanocomposite stabilization requires systems with typically 10^5 – 10^6 atoms, and 10^4 – 10^5 vacancy jumps per atom. For that reason, we instead consider an immiscible $\text{A}_{50}\text{B}_{50}$ generic alloy with kinetics and energetics comparable to $\text{Ag}_{50}\text{Cu}_{50}$.

A description of the kinetic model for thermal diffusion can be found in Ref. 3. The A and B atoms occupy sites on a rigid face centered cubic (fcc) lattice, and interact by nearest-neighbor pair interactions e_{ij} . A single vacancy is placed in the system, and the frequency of atom–vacancy exchange is determined using standard rate theory, with the activation energy given by the energy required to break the bonds between the jumping atom and its surrounding, less the energy recovered when the atom is placed at the saddle point position. Time evolution is determined by a residence-time algorithm,²¹ where the frequency of vacancy exchanges is weighted against the frequency of random-atomic relocations. One of the two kinds of events is randomly chosen according to their relative probabilities, and time is updated as the inverse of the sum of the individual frequencies.

The material parameters used in the simulation follow the choices made in Refs. 3 and 5, i.e., $e_{AA}=e_{BB}=-0.7233$ eV, $w_{AB}=2e_{AB}-e_{AA}-e_{BB}=0.05533$ eV, $e_{AV}=e_{BV}=0.255$ eV. The latter parameters are the atom–vacancy ghost interactions, introduced so as to reproduce the proper ratio between the cohesive and vacancy-formation energies in fcc metals.²² The ordering energy w_{AB} corresponds to a heat of mixing $\Delta H_m=8.0$ kJ/g atom, or to a critical temperature of the miscibility gap $T_c=1573$ K. This heat of mixing is close to the calculated (6–8.5 kJ/g atom)^{23–25} and measured (6 kJ/g atom)²³ values for Ag–Cu. The vacancy migrates with an attempt frequency $\nu_0=10^{14}$ s⁻¹, and the migration energy for the pure elements is set at $E_{m,v}=0.8$ eV, values representative of Ag and Cu. In the results presented here, the temperature has been kept constant at 400 K, as this is the temperature where nanocomposite formation has been observed experimentally in Ag–Cu during 1 MeV irradiation.⁸

The effect of ion-beam processing on the composition field of the alloy is modeled by introducing forced atomic relocations at a controlled frequency per atom Γ . In our model, we randomly select an atom and a jump distance, in compliance with the distribution of atomic relocations obtained by MD, for the given ion. Since KMC simulations are based on a fixed lattice, the data from MD are first lumped

into different neighboring shells. Once the distance is selected, a random direction in space is chosen, and the closest lattice point to that location is the final destination of the relocating atom.

For realistic modeling, the forced exchanges should be introduced correlated in time and space, so as to reproduce the cascade size and density observed in the MD simulations. Such an approach, however, would result in several complications in the KMC simulations, in particular regarding the creation and annihilation of point defects. As we focus here on the role played by the distribution of relocation distances, we simply perform the forced exchanges one at a time in all irradiation cases. Finally, we note that there is presently no evidence that atomic relocation correlations in displacement cascades can, by themselves, lead to compositional patterns, but we leave this point for future work.

The simulation domain is a $L \times L \times L$ rhombohedral crystal with periodic boundary conditions. The faces of the rhombohedron are $\{111\}$ planes in the fcc crystal. For this fcc crystal, we use a_0 to denote the lattice parameter. The simulations reported here are carried out with $L=64$, but to check for finite-size effects we have also performed simulations with $L=32$ and $L=128$. In order to maintain comparable parameters when L is changed, time is rescaled with a reference value for the vacancy concentration $C_v = 1/(64)^3$. In this model, C_v only enters as a multiplicative factor for the time scale of diffusion. The chosen value is comparable to the high-vacancy concentrations that can be generated by irradiation at low temperatures. This quantity can be estimated for specific irradiation conditions using rate equations that include the production, diffusion, and annihilation of point defects. While the principles for performing this modeling are well established,²⁶ an accurate quantitative evaluation is difficult to realize, particularly for the case of a concentrated alloy, since it involves the knowledge of a large number of parameters that cannot be easily estimated *a priori*. These difficulties notwithstanding, to our aid comes the fact that the behavior of the system depends on the *relative* frequency of atomic relocations, that is, the ratio between the frequency of atomic relocations Γ and the thermal mobility, which allows us to interpret the quantitatively unknown vacancy concentration as a change in the time scale, i.e., a rescaling of the relative irradiation intensity.

Consequently, while the present results are obtained by fixing the irradiation temperature and varying the frequency of forced atomic exchanges Γ , the same sequence of steady states is obtained by fixing Γ and varying the temperature.⁵ The former scheme is somewhat easier to implement in the simulations, while the later scheme would be easier to carry out experimentally.

III. RESULTS

A. Distributions of atomic relocation range

The primary recoil spectra are displayed in Fig. 1 for the four ions considered, given as the total number of atoms displaced for one incoming ion at all depths. Note that the He distribution is shifted to lower energies, with the maximum kinetic energy transfer to Ag and Cu atoms being only

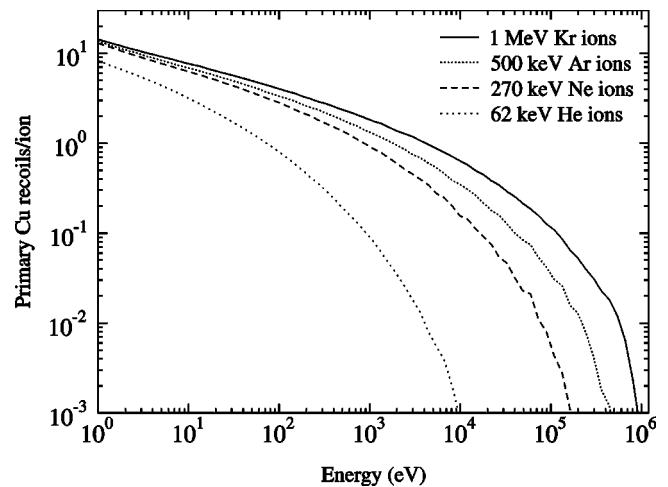


FIG. 1. Number of primary Cu recoils produced by one incoming noble gas ion at all depths. The corresponding curves for Ag recoils are qualitatively similar, and quantitatively do not differ much from the Cu curves, so these are omitted for clarity. The curves are averages over 10^4 – 3×10^4 range simulations of ions impacting on different surface positions.

8–14 keV, in comparison to 140–980 keV for the other ions. In Fig. 2 we show the distributions of atomic relocations for each energetic ion (He^+ , Ne^+ , Ar^+ , or Kr^+) extracted from the MD simulations. As expected, the total number of relocations increases significantly with the projectile mass. In addition, peaks are observed for small relocation distances; the first peak, at $d=0$ Å, corresponds to atoms that have not been relocated, as they are still on the site that they occupied before irradiation, although they have been slightly displaced; the following peaks at 2.7, 3.9, and 4.7 Å correspond to atoms that have been relocated to first, second, and third nearest neighbor sites, respectively. For distances larger than 8 Å, peaks are no longer resolved, as the separation distances between consecutive neighboring shells become comparable to the displacements between actual relaxed atomic positions and perfect lattice positions. This produces smooth tails for $d > 8$ Å for Ne, Ar, and Kr irradiations. For He, the small relative number of large displacements results in insufficient statistics to obtain a smooth tail. The main point here is that Ne, Ar, and Kr irradiation produces a long-range tail in the

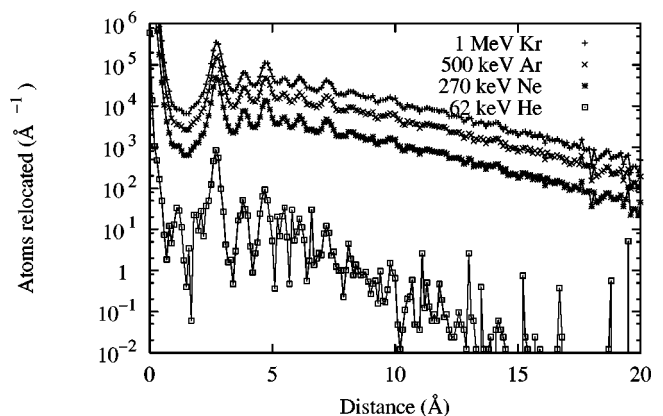


FIG. 2. Atomic relocations produced by the collision cascades initiated by the indicated ions on a $\text{Ag}_{50}\text{Cu}_{50}$ alloy.

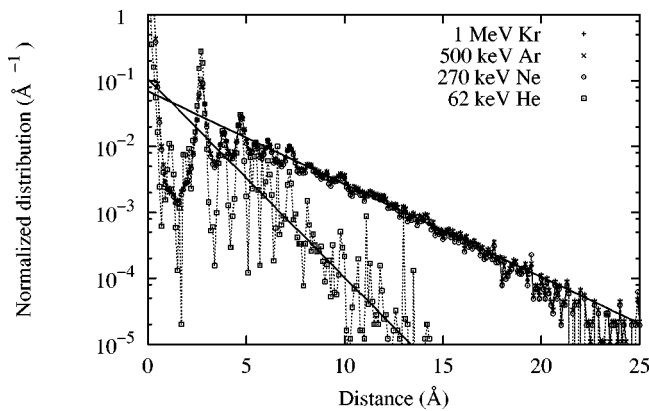


FIG. 3. Normalized distributions of atomic relocations. Ne, Ar, and Kr give essentially the same normalized distribution. He, on the other hand, produces a relocation distribution that weighs short-range jumps more heavily. Also shown are fittings to the data based on exponential decays: $0.07 \text{ \AA}^{-1} \exp(-r/3.08 \text{ \AA})$ for the case of Ne, Ar, and Kr, and $0.08 \text{ \AA}^{-1} \exp(-r/1.44 \text{ \AA})$ for the case of He.

atomic relocation range distribution, whereas He irradiation involves only short-range mixing. The long-range tails, as we will show, play a critical role in the stabilization of compositional patterns.

Aside from the variation in the total number of relocations, which increases from 4.64×10^4 , to 1.75×10^5 , to 4.21×10^5 for Ne, Ar, and Kr ions, respectively, these three ions produce very similar distributions. The similarity in the distributions for Kr, Ar, and Ne is illustrated explicitly in Fig. 3, where the normalized distributions are plotted. In the analysis that follows, therefore, we will treat the case of irradiation by 1 MeV Kr as representative of the general behavior for the three heavy ions. The distribution for He, on the other hand, is qualitatively different, and only 298 atoms are relocated for each incoming ion. For all the ions, we find that the atomic relocations can be assumed to be homogeneously distributed along the trajectory of the ion. The distribution remains essentially unchanged if we used the recoil spectrum for the ions along their whole trajectory, or only while they travel between 50 and 150 nm inside the material.

B. Steady-state microstructures under irradiation

The above distributions of atomic relocations are next fed into the KMC simulations. To that effect, the data are first lumped into neighboring shells. Figure 4 shows a comparison between the data lumped from MD, which is an input for the KMC simulations, and the distribution actually generated in the KMC code by the method described in the previous section. We note that the latter present greater oscillations with respect to the mean curve. These oscillations result from the large variation of coordination numbers from neighboring shell to neighboring shell on a rigid lattice, which introduces a bias in the probability to relocate atoms on these shells. This bias is much less pronounced in the MD results since, due to lattice relaxation, there is a spreading of the distance distribution, instead of sharply defined peaks.

For each ion, a series of simulations is performed to determine the sequence of steady states reached as the forced relocation frequency Γ is increased. We verified that the true

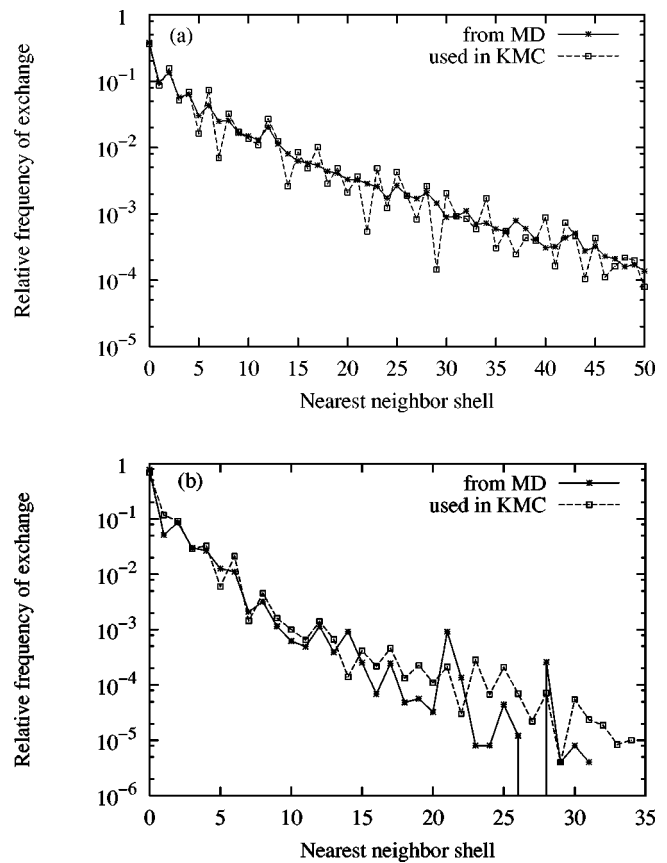


FIG. 4. Comparison between the distribution of atomic relocations calculated by MD, (lumped into the discrete jumps on a fixed fcc lattice), and the ones actually used in the KMC simulations: (a) 1 MeV Kr and (b) 62 keV He.

steady state is obtained under the chosen conditions by checking that simulations with two extreme initial states, a random solid solution and a pure A/B bilayer, resulted in statistically identical results. As recalled in Sec. I, steady-state patterning takes place when the forced relocations are sufficiently frequent to prevent macroscopic decomposition, but not as high as to force a solid solution. A first glimpse of the nature of the steady states is obtained by direct visualization of the configurations. As discussed in a previous article,⁵ this qualitative assessment is not always sufficient to distinguish patterned microstructures from solid solutions. For an unambiguous determination, we calculate the spherically averaged structure factor $S(k)$ of these configurations: in the case of a solid solution $S(k)$ decreases monotonously with k , adopting a shape close to a Lorentzian; in a patterned state, on the other hand, $S(k)$ contains a peak at some nonzero wave vector k .

Figure 5 displays a sequence of steady states obtained with the Kr relocation distribution. The stabilization of patterns is clear, and it is confirmed by the corresponding structure factors, shown in Fig. 6. No attempt is made here to precisely determine the stability boundaries from macroscopic decomposition to patterning, and from patterning to solid solution, as Γ increases. As discussed in Ref. 5, these boundaries are difficult to determine accurately in the KMC

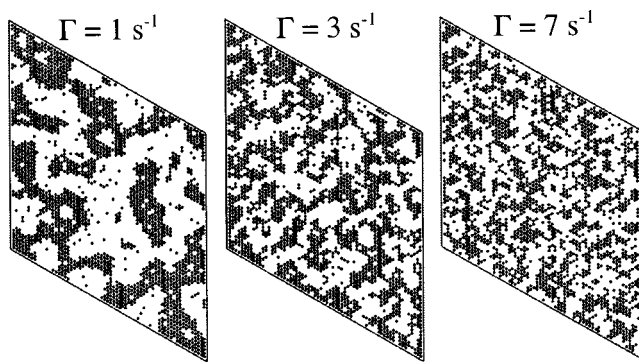


FIG. 5. A series of steady-state microstructures from KMC simulations based on the distribution of atomic relocations produced by 1 MeV Kr ions. Two-dimensional cuts of the three-dimensional simulations. We can observe the formation of steady-state patterns with a characteristic length scale, in a nanocomposite structure.

simulations due to finite size effects and to atomic correlations in the solid solutions, respectively.

In the case of He irradiation (Fig. 7), patterns are not visually observed in the microstructures. Furthermore, the required peak in $S(k)$ for patterning is also absent (Fig. 8), even after refining the spectrum of Γ values. We can therefore conclude that patterning does not take place in the KMC simulations when the relocation distribution for He irradiation is used.

IV. DISCUSSION

The main purpose of this article is to address, by simulations, the effect of the primary recoil spectrum on the microstructural evolution in Ag–Cu thin films. Previous work has shown that stable nanocomposites form if the average recoil distance of displaced atoms is sufficiently large. The present simulations examine whether such relocation distributions can be realized in real systems, and under what irradiation conditions. Here we considered the primary recoil spectra of He, Ne, Ar, and Kr ions in Ag₅₀Cu₅₀. The energies of the ions were chosen to maximize the damage energy in

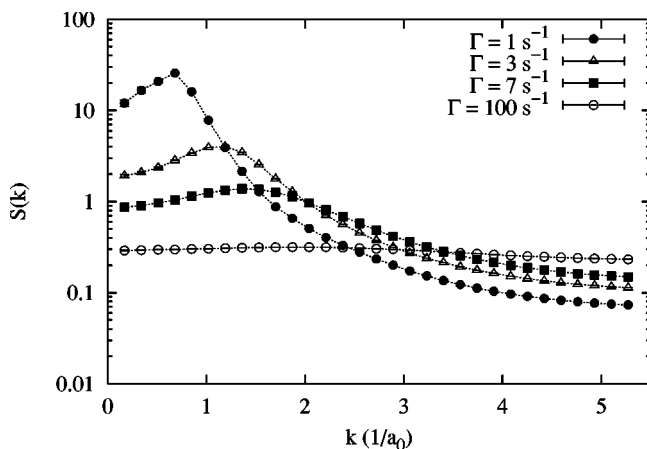


FIG. 6. Structure factor for the microstructures shown in Fig. 5, plus a curve for a high frequency of random relocations $\Gamma = 100 \text{ s}^{-1}$, corresponding to a solid-solution microstructure.

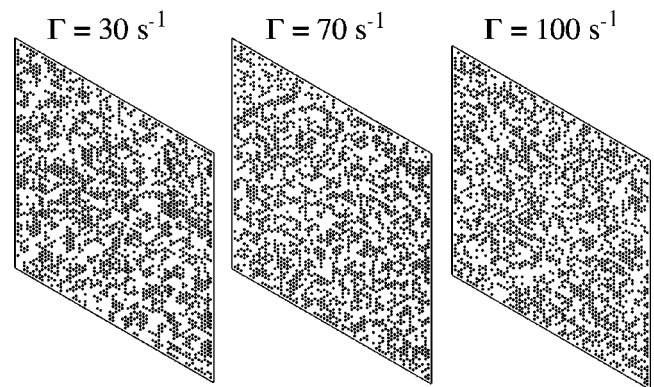


FIG. 7. A series of steady-state microstructures from KMC simulations based on the distribution of atomic relocations produced by 62 keV He ions.

200 nm thick films for possible future comparison with experiment. Note, however, that the primary recoil spectrum is quite insensitive to ion energy.

When the distributions of atomic relocations for all the ions are normalized, we find two paradigmatic cases: irradiation by “heavy” ions (Ne, Ar, and Kr) and “light” ions (He). The heavy ion displacement distributions are nearly identical in shape (Fig. 3) because they produce a large number of recoils with energies higher than 10 keV. Only these high-energy recoils can produce long-range atom relocations. Moreover, at energies somewhat above 10 keV, cascades in Ag–Cu are split into subcascades,¹⁹ making the atom redistribution self similar. Hence the tails of the heavy ion atom displacement distributions (Figs. 2 and 3) are similar.

Let us first discuss in some detail the displacement distribution of Kr irradiation. In this case, the long-range tail of the distribution is well fitted by an exponential decay with a decay length of $\approx 3.08 \text{ \AA}$, as shown in Fig. 3. The actual functional form for the distribution of atomic relocations, however, deserves a closer examination: even though our KMC simulations are not based on these functional forms, this analysis is still of relevance to theoretical models, such as those developed in Refs. 4 and 12. Furthermore, it can shed light on the physical mechanism underlying forced

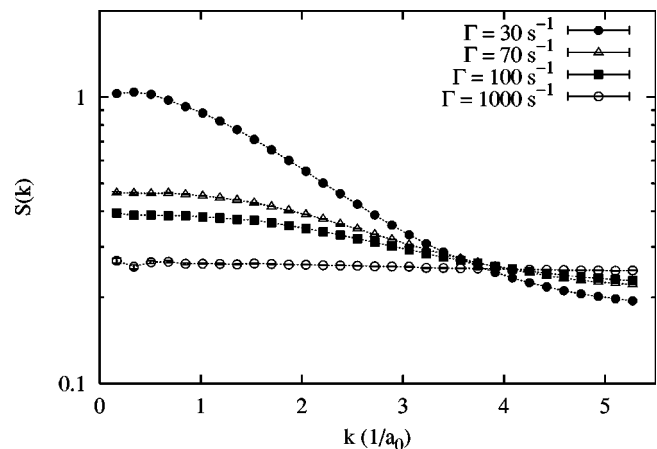


FIG. 8. Structure factor for the microstructures shown in Fig. 7, plus a curve for a high frequency of random relocations $\Gamma = 1000 \text{ s}^{-1}$, corresponding to a solid-solution microstructure.

atomic relocations, helping to determine whether long-range mixing is mainly ballistic or takes place during the thermal spike.²⁷ To address this point let us consider two models based on the possible physical scenarios: (1) atomic relocations are produced via a random walk in the thermal spike; and (2) atomic relocations are ballistic and thus distributed according to an exponential decay, which is characterized by the atom mean-free path. The corresponding distributions of relocation distances after spherical averaging are, in the first case, a Gaussian distribution

$$W_R^{(1)}(r) = A_1 r^2 \exp(-3r^2/2R_1^2),$$

and in the second case, an exponential decay

$$W_R^{(2)}(r) = A_2 r^2 \exp(-r/R_2). \quad (1)$$

In these equations R_1 and R_2 are the average random walk distance and the mean-free path, respectively. Therefore, to test the measured distributions against these two models, we can use the generic fitting function

$$W_R(r) = A r^n \exp(-r^n/R), \quad (2)$$

where A , n , and R are fitting parameters. Only the quasicon- tinuum part of the actual distributions is used for this fitting ($5 \text{ \AA} < d < 19 \text{ \AA}$). We find that the set of parameters that fit the data are $A = 44\,000 \text{ atom/\AA}$, $R = 1.27 \text{ \AA}$, and $n = 0.87$. The fitted value for n makes this exponent far closer to an exponential tail than to a Gaussian profile. Instead of using n as a parameter, we can also attempt to fit the data by fixing $n = 1$ and $n = 2$. We find that a good fit is obtained with $n = 1$, as it can be seen in Fig. 3. However, the Gaussian profile with $n = 2$ fails to reproduce the behavior of the data, reinforcing the idea that long-range relocations are mainly of a ballistic nature.

The observation that the tail of the relocation distribution agrees better with a ballistic relocation model than with a heat spike model might at first seem surprising, since cascades in Ag–Cu are well known to be in the heat spike regime for recoil energies higher than $\sim 5 \text{ keV}$ (see Refs. 18 and 28). The atom relocations that occur in the heat spike, however, are relatively short range, since the liquidlike zone persists for a few picoseconds. Hence the number of relocated atoms in a thermal spike is large but their relocation distance is small. The existence of “ballistic” long-range tails in the displacement distribution is therefore not in contradiction with the nature of atomic mixing in thermal spikes.

We now turn to the 62 keV He irradiation case, for which practically all recoils have energies well below 10 keV (Fig. 1). The redistribution of atoms is dominated by low-energy cascades, and as a result medium- and long-range relocations are rare. The number of events at these lower recoil energies, unfortunately, is too low to perform a statistically meaningful fit. It is nevertheless clear that the He relocation distribution is more concentrated toward short relocation distances, as compared to the distributions produced by Ne, Ar, and Kr ions. If a simple exponential fit is attempted, as shown in Fig. 3, the decay length is $R = 1.44 \text{ \AA}$ which, in fact, is half that obtained for the three other ions.

By KMC simulations we analyze ion-beam mixing in these two cases, and find that while compositional patterning

can be achieved by bombardment with Kr (“heavy”) ions, it cannot be achieved by irradiation with He (“light”) ions. No characteristic length scale can be observed in the structure factor $S(k)$ for the He case, while one is clearly evident in the Kr case. This is due to the larger relocation distances forced by heavy-ion irradiation. In fact, these two cases resemble the model cases examined in Ref. 5, when both situations were encountered by changing the average relocation distance R . The case of He is representative of an atomic mixing by purely nearest-neighbor exchanges, while Kr is representative of mixing involving longer relocations. The present results would indicate that the critical relocation range for compositional patterning lies between ≈ 1.5 and $\approx 3 \text{ \AA}$, assuming exponential decays for the relocation distributions. This is in very good agreement with the continuum theory applied to the model alloy used in the KMC simulations: it predicts a critical relocation range of one half nearest neighbor distance, i.e., 1.38 \AA .⁵

We next compare the results presented here with the ion beam mixing experiments in Ag–Cu.^{8,11} It was mentioned before that a direct quantitative comparison presents difficulties with regards to the exact estimation of the times for diffusion. However, we can still estimate the frequency of atomic relocations in the experimental case by means of the results presented in Fig. 2. In the experiment of ion-beam mixing of Ref. 8 the irradiation flux was $1.21 \times 10^{13} \text{ ion/cm}^2 \text{ s}$, corresponding to an experimental frequency of atomic relocations $\Gamma \approx 2.8 \text{ s}^{-1}$. It is encouraging that this is in agreement, at least within 1 order of magnitude, with the frequencies required to produce patterning in the simulations presented here in Fig. 5.

The KMC simulation results show that in the case of ion-beam mixing with light ions, no length-scale selection is found, as evidenced in the structure factor $S(k)$. The information contained in the structure factor suggests that small angle scattering experiments are the appropriate experimental tool to study the formation of compositional patterns by ion-beam mixing, since different distinct features are present for each ion case. Such experiments have not been performed yet, although they have been previously proposed.^{5,8} A random solid solution synthesized, for instance, by low temperature irradiation would provide a suitable initial state. Based on the idea of using small angle scattering as the characterization technique, we can make an estimation of the total doses required in this experimental procedure by comparing the cases of Kr and He irradiation, as presented in Figs. 6 and 8. From those figures we can establish that an equilibration of the structure factor up to a minimum wave vector $k_{\min} \approx 0.7/a_0$ is necessary to make a clear distinction between both cases. In our KMC simulations, starting from a random solid solution initial condition, we find that He doses in the range $5 \times 10^{16} - 2 \times 10^{17} \text{ ion/cm}^2$ are needed to achieve a steady state in the structure factor evaluated at k_{\min} . These are reasonable doses from the experimental point of view, making it feasible to test the prediction that steady-state compositional patterning cannot be stabilized with 62 keV He irradiation.

V. CONCLUSION

We have studied the influence of the atomic relocation range in displacement cascades produced by light and heavy ions on the composition evolution in a binary alloy under irradiation. We have first determined by molecular dynamics the characteristics of irradiation mixing in a Ag–Cu alloy subjected to bombardment with 62 keV He, 270 keV Ne, 500 keV Ar, and 1 MeV Kr ions. The distributions of atomic relocations measured by MD have then been used to perform lattice KMC simulations of phase evolution. The KMC results have shown that nanoscale steady-state compositional patterns can be stabilized by irradiation with heavy ions (Ne, Ar, and Kr), but not with light ions (He). As the characteristic relocation range for He ions is half that measured for the heavy ions, these results support an earlier theoretical prediction that compositional patterning can take place under irradiation only if the forced atomic relocation range exceeds a critical value.

ACKNOWLEDGMENTS

This research was supported by the University of Michigan, and the U.S. Department of Energy, Division of Materials Sciences, under the Award No. DEFG02-91ER45439, through the Materials Research Laboratory at the University of Illinois at Urbana-Champaign. K.N. acknowledges support from the Academy of Finland under Project No. 73722. Grants of computer time from the center of scientific computing in Espoo, Finland, the National Energy Research Scientific Computing Center, and the National Center for Supercomputing Applications are also gratefully acknowledged.

- ¹P. Chakraborty, *J. Mater. Sci.* **22**, 2235 (1998).
- ²Nanotechnology Research directions: IWGN workshop report, NSF September 1999.
- ³P. Bellon and R. S. Averback, *Phys. Rev. Lett.* **74**, 1819 (1995).
- ⁴R. A. Enrique and P. Bellon, *Phys. Rev. Lett.* **84**, 2885 (2000).
- ⁵R. A. Enrique and P. Bellon, *Phys. Rev. B* **63**, 134111 (2001).
- ⁶F. Wu, P. Bellon, A. J. Melmed, and T. A. Lusby, *Acta Mater.* **49**, 453 (2001).
- ⁷S. Zghal, R. Twesten, F. Wu, and P. Bellon, *Acta Mater.* **50**, 4711 (2002).
- ⁸R. A. Enrique and P. Bellon, *Appl. Phys. Lett.* **78**, 4178 (2001).
- ⁹T. Klassen, U. Herr, and R. S. Averback, *Acta Mater.* **71**, 2821 (1997).
- ¹⁰B. Y. Tsaur, S. S. Lau, and J. W. Mayer, *Appl. Phys. Lett.* **36**, 823 (1980).
- ¹¹L. C. Wei and R. S. Averback, *J. Appl. Phys.* **81**, 613 (1997).
- ¹²K.-H. Heinig, B. Schmidt, M. Strobel, and H. Bernas, *Mater. Res. Soc. Symp. Proc.* **650**, R9.6 (2000).
- ¹³B. Schmidt, K.-H. Heinig, and A. Mücklich, *Mater. Res. Soc. Symp. Proc.* **647**, 011.20 (2000).
- ¹⁴G. C. Rizza, M. Strobel, K.-H. Heinig, and H. Bernas, *Nucl. Instrum. Methods Phys. Res. B* **178**, 78 (2001).
- ¹⁵R. S. Nelson, J. A. Hudson, and D. J. Mazey, *J. Nucl. Mater.* **44**, 318 (1972).
- ¹⁶K. Nordlund, *Comput. Mater. Sci.* **3**, 448 (1995).
- ¹⁷S. M. Foiles, M. I. Baskes, and M. S. Daw, *Phys. Rev. B* **33**, 7983 (1986).
- ¹⁸T. J. Colla, H. M. Urbassek, K. Nordlund, and R. S. Averback, *Phys. Rev. B* **63**, 104206 (2000).
- ¹⁹K. Nordlund, L. Wei, Y. Zhong, and R. S. Averback, *Phys. Rev. B* **57**, 13965 (1998), and references therein.
- ²⁰J.-L. Bocquet, *Defect Diffus. Forum* **203–205**, 81 (2002).
- ²¹G. Martin and P. Bellon, *Solid State Phys.* **50**, 189 (1997).
- ²²Doyama and Koehler, *Acta Metall.* **24**, 871 (1976).
- ²³R. Najafabadi, D. J. Srolovitz, E. Ma, and M. Atzmon, *J. Appl. Phys.* **74**, 3144 (1993).
- ²⁴M. Asta and S. Foiles, *Phys. Rev. B* **53**, 2389 (1995).
- ²⁵V. Ozolins, C. Wolverton, and A. Zunger, *Phys. Rev. B* **57**, 6427 (1998).
- ²⁶R. Sizman, *J. Nucl. Mater.* **69/70**, 386 (1978).
- ²⁷P. Sigmund and A. Gras-Marti, *Nucl. Instrum. Methods* **182/183**, 25 (1981).
- ²⁸T. Diaz de la Rubia, R. S. Averback, R. Benedek, and W. E. King, *Phys. Rev. Lett.* **59**, 1930 (1987); **60**, 76 (1988).